Progress in Oceanography 245 (2026) 103745

Contents lists available at ScienceDirect

Progress in Oceanography

journal homepage: www.elsevier.com/locate/pocean

In situ and satellite characterization of a meddy north of the Azores: NA-VICE cruise (2012), Azores to Iceland

Tiago Serpa [a,b,c,*], Igor Bashmachnikov [d,e], Paulo Relvas [f], Ana Martins [a,b]

[a] University of the Azores, Institute of Marine Sciences - OKEANOS, Rua Professor Doutor Frederico Machado 4, 9900-140 Horta, Portugal
[b] Department of Oceanography and Fisheries, Faculty of Sciences and Technology, University of the Azores, Rua Prof. Doutor Frederico Machado, 4, 9901-862, Horta, Faial, Azores, Portugal
[c] IMAR, Instituto do Mar, Rua Prof. Dr. Frederico Machado, n.° 4 9900-138 Horta, Faial, Azores, Portugal
[d] St. Petersburg State University, 7-9 Universitetskaya Embankment, 199034 St Petersburg, Russia
[e] Nansen International Environmental and Remote Sensing Centre, 14 Line V.O., 7, 199034 St.Petersburg, Russia
[f] CCMAR, Center of Marine Sciences, University of Algarve, Campus de Gambelas, 8005-139 Faro, Portugal

ARTICLE INFO

Keywords:
Meddies
Mediterranean water
Northeast atlantic
Eddy detection algorithm
Meddy generation sites

ABSTRACT

The influx of Mediterranean Water through the Strait of Gibraltar significantly influences the Northeast Atlantic. This inflow gives rise to distinctive oceanographic features known as Mediterranean Water Eddies (Meddies), which are characterized as deep, anticyclonic lenses of warm, saline water.

During the R/V *Knorr* cruise KN207-03, conducted from the Azores to Iceland in the summer of 2012 as part of the international NA-VICE project, a meddy was identified at 41.3°N, 27.1°W. Its main physical properties were determined using *in situ* measurements from a Conductivity-Temperature-Depth (CTD) profiler and an Acoustic Doppler Current Profiler (ADCP). The meddy exhibited salinity and temperature anomalies of 0.26 and 2.4°C, respectively, along with azimuthal velocities reaching 0.38 m s^{-1}. These characteristics were compared with established criteria from previous studies to confirm that the observed feature – located further north than most previously documented meddies – met the classification requirements.

At the time of the cruise, a cyclonic eddy exhibiting Mediterranean Water characteristics was detected north of the meddy. The analysis suggests that these features interacted, resulting in trapping of Mediterranean Water beneath the cyclone. The meddy sea surface expression was examined using altimetry data combined with an eddy detection algorithm, revealing a Sea Level Anomaly of 14 cm and a radius of 57 km. Additionally, altimetry and Argo data were used to reconstruct the meddy trajectory, indicating that it originated in the Irish continental shelf. This finding supports the hypothesis that meddies can form north of the Iberian Peninsula, as far as the extension of the Mediterranean Outflow.

1. Introduction

Mediterranean Water Eddies (Meddies) are distinct features of the North Atlantic's intermediate depths (Käse & Zenk, 1987). These structures are deep anticyclones composed of warm, saline water characteristic of Mediterranean Water (MW), which is transported over large distances, contributing to the heat and salt budget of the North Atlantic (Armi et al., 1989; Armi & Zenk, 1984; Richardson et al., 1989). This contribution occurs through the dissipation and destruction of meddies along their pathways (Armi et al., 1989; Richardson et al., 2000) and accounts for approximately 50% of the MW's salt flux into the Atlantic (Arhan et al., 1994), highlighting their significant climatic role. However, due to the challenges associated with deep-ocean observations, meddies remain only partially understood, and direct measurements are limited.

North Atlantic Central Water (NACW) and MW interact at the Strait of Gibraltar, where the former enters the Mediterranean at the surface while the latter exits at depth. This two-layer exchange results from density differences, as MW is denser due to excess evaporation over precipitation and river runoff in the Mediterranean basin (Ochoa & Bray, 1991). Upon exiting the strait, MW sinks along the continental slope, entraining NACW until it reaches a neutrally buoyant depth of

* Corresponding author at: University of the Azores, Institute of Marine Sciences - OKEANOS, Rua Professor Doutor Frederico Machado 4, 9900-140 Horta, Portugal.
E-mail addresses: tiago.l.serpa@uac.pt (T. Serpa), igorb1969@mail.ru (I. Bashmachnikov), prelvas@ualg.pt (P. Relvas), ana.mp.martins@uac.pt (A. Martins).

https://doi.org/10.1016/j.pocean.2026.103745
Received 27 January 2026; Received in revised form 13 April 2026; Accepted 17 April 2026
Available online 18 April 2026

approximately 1000 m, forming the Mediterranean Outflow Water (MOW) (De Pascual-Collar et al., 2019). As it spreads through the Gulf of Cadiz, MOW reaches equilibrium and bifurcates into two branches due to interactions with bottom topography and mixing: an upper branch at 500–800 m depth and a lower branch at 800–1200 m depth (Gasser et al., 2017). Ambar et al. (2002, 2008) identified these branches as cores of maximum temperature and salinity and additionally described a third, shallower core at depths shallower than 600 m.

Within the Gulf of Cadiz, MOW is characterized by temperatures of 13.6–13.7°C and absolute salinities (SA) of 37.1–37.4 g kg^{-1}, depending on depth within its upper and lower branches (Gasser et al., 2017). After passing Cape São Vicente, MOW turns northward along the western Iberian margin as the Mediterranean Undercurrent (MUC), where it becomes trapped in the Tagus Basin and circulates anticyclonically (Daniault et al., 1994). From this region, it follows two primary pathways: one extends poleward along the western European continental slope, reaching the Bay of Biscay and continuing northward to the Porcupine Bank and Rockall Trough at 53°N, while the other propagates westward toward the Mid-Atlantic Ridge (MAR) (De Pascual-Collar et al., 2019). As MOW mixes with surrounding water masses, its temperature decreases, reaching values exceeding 10°C at 800 m and 7°C between 800–1400 m depth in the Bay of Biscay (Bower et al., 2002). These characteristics are largely attributed to the lower MOW core, which exhibits potential temperature values of 8–12°C and practical salinities (SP) of 35.6–35.9 at 1000–1100 m depth (Iorga & Lozier, 1999a, 1999b). For reference, the relationship between SA and SP in the North Atlantic is given by SA = SP + 0.16504 g kg^{-1} (McDougall et al., 2012). In addition to these primary pathways, MOW also spreads southward and southwestward, transported by MW lenses (Armi & Zenk, 1984).

Meddy detection requires *in situ* data to characterize their structure and distinguish them from the surrounding ocean. This involves computing their salinity and temperature anomalies relative to the ambient background. Consequently, meddy research is highly dependent on deep-ocean monitoring. Since the first observations, studies have utilized hydrographic surveys, floats, and mooring stations to study meddies (Arhan et al., 1994; Armi et al., 1989; Armi & Stommel, 1983; Armi & Zenk, 1984; Käse & Zenk, 1987; Pingree & Le Cann, 1993b; Prater & Sanford, 1994; Richardson et al., 1989; Richardson & Tychensky, 1998). When float observations or hydrographic surveys do not allow for gridded sampling, climatological datasets representing the region's ambient characteristics are often employed.

Observational data have been incorporated into numerical models, significantly improving the understanding of meddy formation and dynamics (Hogg & Stommel, 1990; Jungclaus, 1999; Maas & Zahariev, 1996; Mcwilliams, 1984). A breakthrough in meddy studies occurred in the early 1990 s when Stammer et al. (1991) used satellite altimetry to detect meddies for the first time, identifying their presence through isolated positive anomalies in Sea Surface Height (SSH). In the same decade, Pingree & Le Cann (1993a) used infrared (IR) satellite imagery to observe a meddy, pioneering remote sensing approaches for meddy detection. Subsequent studies expanded these methodologies, utilizing Sea Surface Temperature (SST) data (Oliveira et al., 2000) and satellite altimetry (Bashmachnikov et al., 2013; Bashmachnikov, Machín, et al., 2009; Bashmachnikov, Mohn, et al., 2009; Bashmachnikov, Neves, Calheiros, et al., 2015; Ienna et al., 2014, 2022).

Meddies are characterized by lens-shaped anomalies in salinity and temperature, corresponding to MOW signatures. Their salinity and temperature anomalies can reach 1 and 4°C, respectively, compared to background values (Richardson et al., 2000). They primarily rotate anticyclonically, with azimuthal velocities of up to 30 cm $s^{-}1$, diameters ranging from 40–150 km, and westward propagation speeds of 1–3 km $day^{-}1$ (Richardson et al., 1991, 2000). Their average lifespan is 1–2 years, though some can persist for 4–5 years depending on their decay rate and trajectory, which determines whether they gradually dissipate into the surrounding water or collide with seamounts and disintegrate (Ienna et al., 2014; Richardson et al., 2000). However, meddy dissipation due to seamount collisions depends on the capacity of ambient currents to redirect meddies toward these topographic features in a destructive manner (Bashmachnikov, Mohn, et al., 2009).

The leading theory explaining the formation mechanism of meddies is that they form through baroclinic instability of the MUC along with relative vorticity generated from friction with the bottom (i.e., continental slope) and later detach due to bottom topography, which causes rapid changes in direction (Barbosa Aguiar et al., 2013; Bashmachnikov, Neves, Calheiros, et al., 2015).

Meddies can be classified based on their formation site, pathway, and lifespan. They are categorized as northern or southern meddies, depending on whether they form north or south of the Estremadura Promontory (Barbosa Aguiar et al., 2013; Bashmachnikov, Neves, Calheiros, et al., 2015; Serra & Ambar, 2002). Northern meddies occur three times less frequently than southern meddies and exhibit higher relative vorticity, smaller radii, and stronger buoyancy frequency anomalies (Bashmachnikov, Neves, Calheiros, et al., 2015). Meddies follow three main westward pathways extending toward the MAR—southern (34–36.4°N), central (37.5–41°N), and northern (41–45°N)—as well as a coastal pathway along the northwest African margin toward the Canary Islands (Bashmachnikov, Neves, Calheiros, et al., 2015). These pathways may experience meddy convergence and exchange, influenced by topography and oceanic currents (Bashmachnikov, Neves, Calheiros, et al., 2015).

By analyzing the difference between the peak salinity of a meddy core and the salinity of its nearest MOW point, Bashmachnikov, Neves, Calheiros, et al. (2015) inferred whether meddies were locally generated or advected. Their findings indicated that northern meddies exhibited lower core peak salinity than southern meddies due to the progressive entrainment of fresher ambient water as MOW moves northward. Based on these observations, the authors determined that peak salinity values exceeding 36.3 were characteristic of southern meddies, whereas values below 36.2 indicated northern meddies. Additionally, their study demonstrated that when two meddies merged, their radius and thickness increased, their azimuthal velocity decreased, yet their core salinity remained conserved.

A distinctive aspect of meddy dynamics is their frequent interaction with subsurface cyclonic eddies. While there is no consensus on whether deep cyclonic eddies transporting Mediterranean Outflow Water (MOW) should be classified as meddies, they contribute significantly (30%) to the advection of salt and heat into the North Atlantic (Barbosa Aguiar et al., 2013). Whereas most meddies are found in the lower MOW branch at approximately 1000 m depth, deep cyclonic eddies are typically located in the shallow branch at around 600 m and propagate northwestward (Barbosa Aguiar et al., 2013). The interaction between anticyclonic and cyclonic meddies has been characterized as a baroclinic dipole, in which both eddies influence each other's motion and size, exchange water along their peripheries, and originate from a shared generation site (Carton et al., 2002; Richardson et al., 2000).

Over the past three decades, satellite altimetry has proven to be a powerful and reliable tool for studying the sea surface expression of meddies. As a meddy propagates, it compresses the water column ahead of it, inducing anticyclonic rotation due to the conservation of potential vorticity and causing isopycnals to rise (Ienna et al., 2022). This isopycnal uplift extends to the surface, leading to an increase in sea surface height (SSH) (Bashmachnikov et al., 2013; Ienna et al., 2022). The intensity of a meddy sea surface expression increases at higher latitudes and is strongly influenced by the surrounding environment, which can result in a partial decoupling between surface expression and the meddy core properties (Ienna et al., 2022). Environmental factors play a crucial role in this process, as meddy core characteristics diminish with increasing distance from their formation site (Richardson et al., 2000), while their surface expression becomes more pronounced westward, accompanied by an increase in radius (Ienna et al., 2022).

Satellite altimetry is thus a feasible tool for tracking meddies

throughout their lifespan, allowing for both forecasting and hindcasting of their trajectories (Bashmachnikov et al., 2013; Bashmachnikov, Machín, et al., 2009), while keeping in mind two problematics: the dependency on *in situ* data to distinguish meddies from other mesoscale features (i.e.: mesoscale eddies, Rossby waves) and the interference from ambient currents and eddies which affect their surface expressions.

In the summer of 2012, the North Atlantic Virus Infection of Coccolithophores Expedition (NA-VICE) (cruise KN207-03 from the Azores to Iceland, Fig. 1) took place aboard the R/V *Knorr* within the framework of the international project *Lipid Lubrication of Oceanic Carbon and Sulfur Biogeochemistry via a Host-Virus Chemical Arms Race* (Ref: OCE-1061883). Data collected during this cruise provided an opportunity to describe a meddy detected at 41.3°N, 27.1°W, coupled with a surface cyclonic eddy of positive salinity and temperature anomalies at 42.9°N, 27.2°W. This study aims to characterize the physicochemical properties of these eddies using *in situ* and altimetry data while tracking them.

2. Methodology

2.1. NA-VICE cruise

During the NA-VICE cruise KN207-03, the R/V Knorr departed from São Miguel harbor, Portugal, en route to Reykjavik, Iceland (Fig. 1). A total of 196 CTD profiles were collected between 37°–65°N and 21°–35°W across 98 stations, with both upward and downward casts. While most profiles reached maximum depths of 150–300 m, seven stations extended to 1500–2000 m. Among these, two stations - 20,703,004 (hereafter referred to as station 4) and 20,703,012 (hereafter referred to as station 12) – were identified for their association with eddies. The R/V Knorr was also equipped with a hull-mounted ADCP and a rosette system for water sampling. This study focuses exclusively on CTD and ADCP data. All datasets from this cruise are publicly available at https://www.rvdata.us/search/cruise/KN207-03.

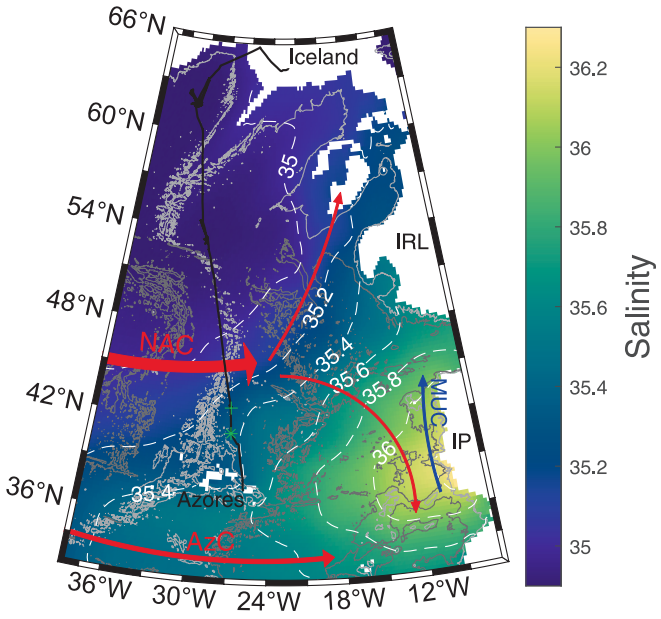

Fig. 1. Track of the NA-VICE cruise KN207-03 aboard the R/V Knorr (black line). The color scheme shows salinity at 1000 m depth, according to the World Ocean Atlas (WOA). Salinity contours are shown in white dashed lines. Bathymetry contours are represented as light gray for 2000 m, and dark gray for 4000 m. Red arrows provide a schematic representation of the main surface currents of the region: North Atlantic Current (NAC), Azores Current (AzC); The blue arrow denotes the Mediterranean Undercurrent (MUC). The locations of stations 4 and 12 (see Section 2.1) are marked as a green asterisk and a green cross, respectively. The main geographic locations are represented: Iceland, Irland (IRL), Iberian Peninsula (IP), and Azores.

The CTD casts were conducted using an SBE 911 Plus system from Sea-Bird Electronics, Inc., equipped with an SBE 43 dissolved oxygen (DO) sensor, and mounted on a rosette system. Measured variables included *in situ* temperature (°C), practical salinity (SP), pressure (dbar), and DO (mL L^{-1}), while density (σ_t) was derived by the CTD.

The Brunt-Väisälä frequency (N) was computed using the Gibbs-SeaWater (GSW) Oceanographic Toolbox for MATLAB. This calculation relied on Absolute Salinity (SA), Conservative Temperature (CT) (both derived through GSW Toolbox functions), and sea pressure (assumed as absolute pressure of 10.1325 dbar). The function used for this computation is based on an equation from the TEOS-10 Manual (McDougall & Barker, 2011) where: $N = \sqrt{g^2 \rho \frac{\beta^{\Theta} \Delta S_A - \alpha^{\Theta} \Delta \Theta}{\Delta P}}$. In this equation, ΔS_A and $\Delta \Theta$ represent the differences in SA and CT between vertically adjacent seawater parcels, separated by a pressure difference (ΔP), measured in pascal (Pa). The density (ρ), saline contraction coefficient (β^{Θ}), thermal expansion coefficient (α^{Θ}), and gravitational acceleration (g) were computed using GSW Toolbox functions.

The presence of a meddy was confirmed by applying criteria from previous studies. The first criterion, proposed by Richardson et al. (1991), specifies that the meddy core should be located between 500–1500 m depth, with a salinity anomaly greater than 0.2, extending over a 200 m layer. Later, Bashmachnikov, Neves, Calheiros, et al. (2015) introduced two additional criteria to their methodology: a maximum temperature anomaly at mid-depths exceeding 0.5°C and a negative buoyancy frequency anomaly within the meddy core.

Anomalies were computed using the MEDTRANS dataset (https://www.mare-centre.pt/en/research/data-library/medtrans-data), which provides the most recent climatology of temperature and salinity distributions in the Subtropical Northeast Atlantic (25–45° N and 6–35° W) with a vertical resolution of 25 m and a horizontal resolution of 30 km (Bashmachnikov, Neves, Nascimento, et al., 2015). To determine these anomalies, the closest coordinates from the climatology were identified for the station of interest, and the difference was calculated between the profile values at every 25 m depth interval, starting at 50 m, and the corresponding climatology values at the same depths.

Velocity measurements were obtained using a hull-mounted ADCP installed on the R/V Knorr, operating an Ocean Surveyor at 75 kHz in Narrowband mode, which provides higher range and accuracy (Hummon & Firing, 2003) with a depth reach of 800 m. The instrument was set to a sampling frequency of 15 min and a vertical resolution of 10 m. The distance between samples was calculated using the Haversine formula, and the data was filtered to be horizontally spaced by 5 km. For the interpretation of velocity's vertical section, the grid was interpolated so that the ratio between the horizontal and vertical resolutions were approximately f/N, where f represents the Coriolis parameter: $f = 2\omega \sin(\varphi)$, with ω being the angular velocity of the Earth around its axis ($\omega = 2\pi/86400$) and φ the latitude.

2.2. Meddy tracking and validation

Altimetry data were obtained from the Copernicus Marine Environment Monitoring Service (CMEMS), specifically the European Seas Gridded L4 Sea Surface Height and Derived Variables Reprocessed 1993 Ongoing product (Copernicus Marine, 2024). This dataset included Absolute Dynamic Topography (ADT) and Absolute Geostrophic Velocity (zonal and meridional components) with a resolution of 0.125° × 0.125°, covering a period from January 1st, 2009, to June 1st, 2013. This product was selected for its enhanced resolution while effectively encompassing the study region, defined between 30°–8° W and 38°–50° N.

The Angular Momentum Eddy Detection Algorithm (AMEDA) (Le Vu et al., 2018) is a hybrid detection method that combines dynamical and geometrical quantities to identify eddy structures. This algorithm not only detects eddies but also calculates various physical characteristics, including eddy center, dimensions, trajectory, velocity, and Rossby number. Additionally, it tracks merging and splitting events, allowing

for the filtering of eddy structures in a time series. By accounting for these interactions, AMEDA helps mitigate the influence of surrounding eddies on a meddy surface expression.

AMEDA was applied to the altimetry dataset to identify the surface expression of the meddy observed during the cruise and analyze its physical characteristics. The translation velocity was computed using the Haversine formula to calculate the distance between consecutive points, divided by the number of days between them. An initial portion of the track was removed after observing that the algorithm lost the meddy for 53 km, resulting in a translation velocity of 0.6 m s^{-1}. The track of the meddy, along with its shape, radius, and velocity, will be presented in the results section of this work.

The track computed by AMEDA was validated using trajectories recorded by Argo floats. Four Argos found within the study area at the same time as the meddy were analyzed by verifying whether their positions were within 0.5° of the meddy center. The analysis showed that Argo n°6900650 followed the meddy for 1.8 years. Temperature and salinity measurements taken from the float during this period were analyzed following the methodology described in Section 2.1.

To estimate the volume transport (Q) carried by the meddy, the following equation was used, based on Zhang et al. (2014): $Q = 2 \times R \times H \times v$, where R is the average radius along the AMEDA track, H is the vertical extent estimated from the CTD cast at station 4 (the closest high-resolution profile to the core), and v is the average translation velocity.

Salinity volume was computed using the equation from Bashmachnikov, Neves, Calheiros, et al. (2015): $S_v = 0.5(2\pi)^{\frac{3}{2}}\mathrm{erf}(1)^3 S_m H R^2$, where S_m is the maximum salinity of the meddy core.

The heat flux was computed following the equations from Bashmachnikov et al. (2023). Assuming all the Argo profiles within 0.5° of the meddy where inside its core, the integral of temperature over the section was computed as: $T_{int} = R(\sqrt{2\pi}\mathrm{erf}(1/\sqrt{2})T(z) - 2T_{ref})$. The heat flux was then computed as: $q = v\int_{z_{low}}^{z_{up}} C_p \rho T_{int}(z)dz \approx 1.7vR\int_{z_{low}}^{z_{up}} C_p\rho(T(z) - T_{ref})dz$, where C_p = 4200 J C^{-1} kg^{-1} is the specific heat capacity of the ocean water, ρ = 1027 kg m^{-3} is the mean water density, and $T_{ref} = -1.8$°C is the reference temperature. Z_{low} and Z_{up} are the lower and upper limits of the core over which the heat content is integrated.

3. Results

3.1. In situ meddy observations

Analysis of the CTD data revealed that only stations 4 and 12 (see Section 2.1) exhibited increased salinity at depth, indicating a higher contribution of Mediterranean Water. These areas are the primary focus of this study.

The vertical salinity profile at station 4 reveals an increase in salinity between 900 and 1400 m, with a deep salinity maximum of 35.55 at 1050 m (Fig. 2a). Compared to the MEDTRANS climatology (Fig. 3a), the salinity anomaly exceeds 0.20 between 1000 and 1300 m, reaching 0.26 at 1100 m. The temperature anomaly exceeds 2 °C between 750 and 1200 m, with a maximum of 2.4 °C at 900 m (Fig. 3b). The Brunt-Väisälä Frequency (N) indicates enhanced stratification between 800 and 1400 m (Fig. 2b), while the corresponding anomaly (Fig. 3c) shows a relative minimum (negative N anomaly) at 1050 m.

Density and dissolved oxygen profiles (Fig. 2c) indicate a well-mixed water column between 400 and 800 m, overlying a pronounced pycnocline between 800 and 1400 m, where potential density increases from 27.18 to 27.70. An oxygen minimum zone occurs within the same depth range, reaching a minimum concentration of 4.04 mL $L^{-}1$ at 970 m. The depth of the oxygen minimum coincides with the peak salinity anomaly, consistent with the typical MW signature.

At station 12, around 160 km north of station 4, both salinity and temperature profiles exhibit an increase between 700 and 900 m depth (Fig. 2a). The N profile (not shown) indicates increased stratification between 500–800 m and between 900–1000 m. Salinity and temperature reach deep maxima between 840 m and 860 m, respectively.

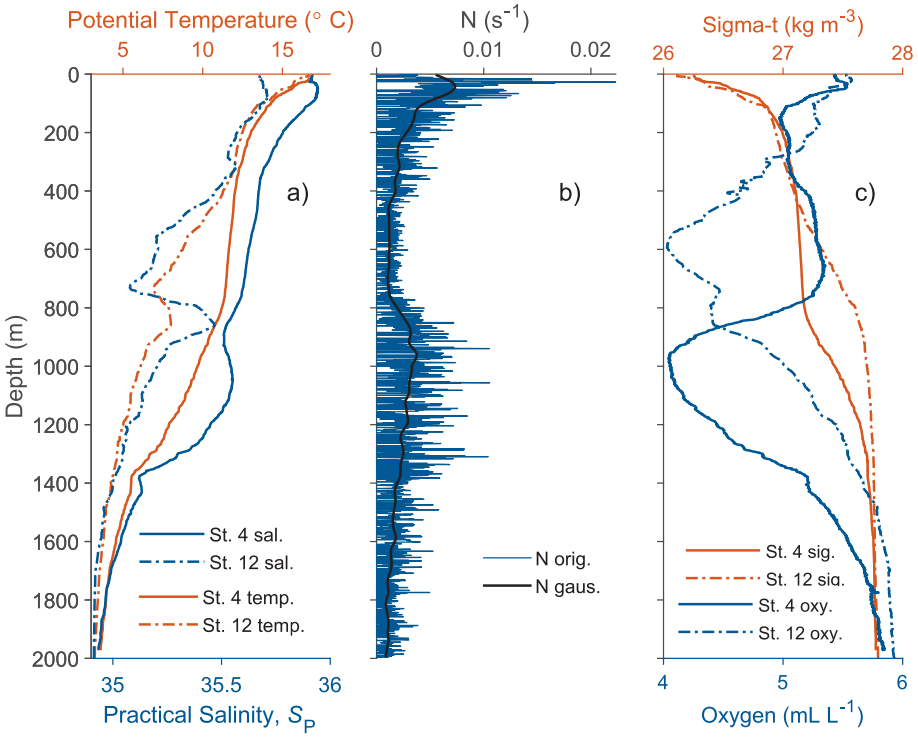

Fig. 2. Vertical profiles of a) temperature (orange) and salinity (blue) for station 4 (solid lines) and station 12 (dashed lines); b) Brunt-Väisälä Frequency (N) for station 4 original data (blue line) and smoothed data using a Gaussian-weighted moving average (black line); c) sigma-t (orange) and dissolved oxygen (blue) for station 4 (solid lines) and station 12 (dashed lines).

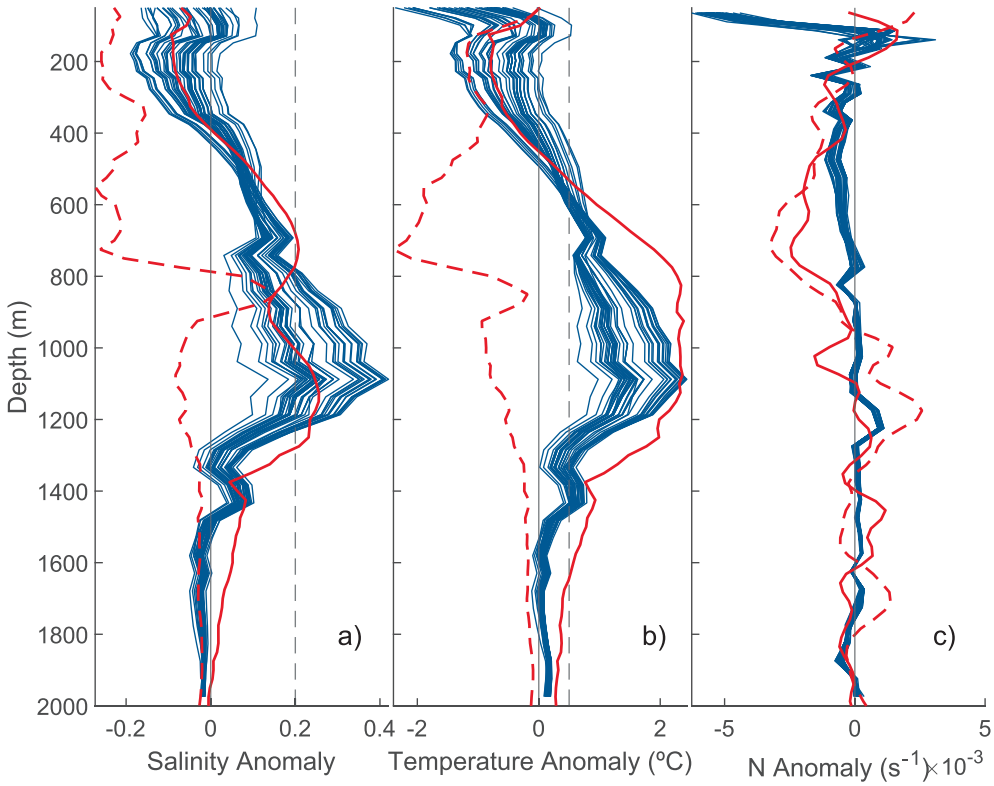

Fig. 3. Vertical profiles of salinity (a), temperature (b), and Brunt-Väisälä Frequency, N (c) anomalies for station 4 (solid red line), station 12 (dashed red line), and Argo Nº 6,900,650 profiles (blue lines) relative to MEDTRANS climatology. Salinity and temperature anomaly of 0.2 and 0.5°C, respectively, are represented as dashed lines for better interpretation of the results.

Relative to the MEDTRANS climatology, the salinity anomaly reached 0.15 (Fig. 3a). Water density steadily rises with depth forming a deep pycnocline between 400 and 800 m (Fig. 2c), just above the deep salinity and temperature maximum. The oxygen concentration reaches a minimum of 4.03 mL L^{-1} at around 600 m, with a secondary minimum of 4.39 mL L^{-1} at the depths of the deep temperature-salinity maximum (Fig. 2c). This deep maximum has properties of the diluted MW. This is demonstrated in the TS-diagram (Fig. 4).

The T-S diagram (Fig. 4) shows that station 4 is characterized by the dominance of NACW in the upper 1000 m. MW dominates between 1050 and 1300 m, while NADW becomes the prevailing water mass between 1800 and 2000 m. Station 12 exhibited characteristics of NACW in the upper 650 m, with MW present between 740 and 910 m, and NADW dominating at approximately 2000 m depth. Station 12 is characterized by colder and less saline water down to around 750 m depth. Water properties suggest a presence of the SAIW in the lower part of this layer. Between 750 and 900 m, the MW influence is well pronounced, bringing water properties of station 12 close to those of station 4 at the same depths. At greater depths, a transition to NADW is evident, marked by a decrease in temperature to less than 4°C below 1800 m.

Summarizing the above, the thermohaline criteria (Bashmachnikov, Neves, Calheiros, et al., 2015; Richardson et al., 1991) suggest the presence of a meddy core at station 4. A weak influence of this meddy may also be detected 160 km away at station 12, presumably below another dynamic structure affecting the upper 50-m layer.

The vertical temperature profiles are complemented with hull-mounted ADCP data, collected along the ship track (Fig. 5). The zonal velocity component clearly reveals the clockwise rotation characteristic of anticyclones associated with the meddy core below 400 m depth, as well as the anticlockwise circulation associated with a surface cyclone, where velocity increases toward the sea surface. The maximum current velocity within the meddy reached 38 cm s^{-1} at approximately 700 m depth. Above the meddy, in the upper 400 m, the rotation axis shifts approximately 5 km along the ship track, and the radius of the maximum velocity increases from 31 km to 90 km. Similar structures have been reported in previous studies (Bashmachnikov et al., 2013) and are characteristic of surface manifestation of meddies (Bashmachnikov et al., 2014; Ienna et al., 2022). The meridional velocity component does not exhibit a well-defined alternating pattern throughout the meddy region, suggesting that the meridional ship track crossed the eastern flank of the meddy core. The cyclonic eddy, located between 550 and 700 km along the track, is also distanced from its center, which contributes to the weak expression of the meridional velocity field. The cyclonic eddy interacts with the meddy and its anticyclonic surface signal, and the rotating structures of these eddies nearly merge.

3.2. *Satellite and Argo*

In the Sea Level Anomaly (SLA) map for June 16 of 2012, the date when the cruise passed station 4 (Fig. 6), it is clearly seen that that ship crosses the anticyclonic structure, identified as the surface signal of the meddy in Fig. 2, practically through its center (about 10 km to the east), while the center of the surface cyclone to the north remained northeastwards of the ship track, about 20 km apart. This confirms the concussions above, derived from the ADCP data. The SLA over the meddy reached 14 cm, while the eddy shape, computed using AMEDA, suggests a mean radius of 57 km. The cyclone shows a comparable SLA of −12 cm and a radius of 61 km.

To put the local velocity field, shown in Fig. 5, into a larger framework, the ADCP data along the ship track between 38 and 64°N were averaged in vertical in the layers 0–400 m and 400–800 m and plotted against latitude (Fig. 7). Throughout the track covering a latitude of circa 26°, 83% of measurements of the current velocity are within 25 cm s^{-1}. The increase of the absolute values with velocities reaching over 30 cm s^{-1} throughout the sampled part of the water column is first observed between 41° and 44°N, where the meddy and a cyclonic structure are

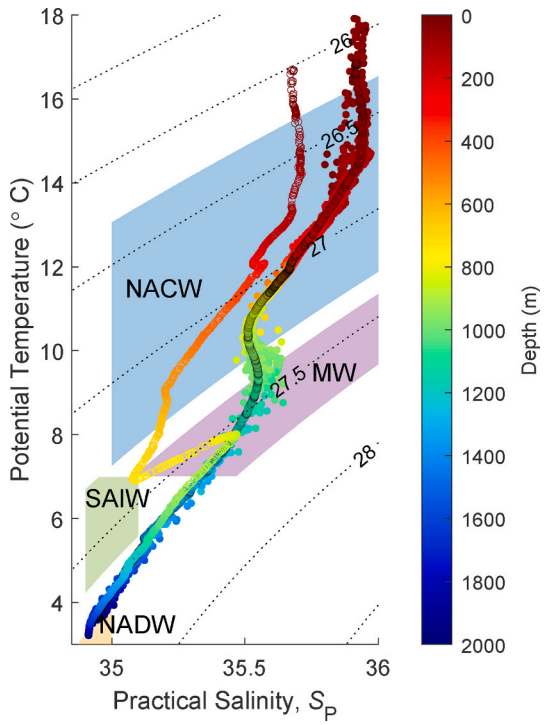

Fig. 4. T-S diagram with vertical profiles of station 4 (circles with black boundary), station 12 (open circles), and Argo profiles (filled circles). Density is represented as black dotted lines. The color bar shows the depth of each point. Different colored areas represent the limits of the water masses (NACW – North Atlantic Central Water; MW – Mediterranean Water; SAIW – Sub-Artic Intermediate Water; NADW – North Atlantic Deep Water) according to temperature, salinity, and density.

present. Between 51°–52.5°N, the velocity in the surface layer increased, showing two peaks reaching over 30 and 40 cm s^{-1}. This location coincides with a branch of the NAC. An increase in the current velocity at 53°–55°N indicates the presence of a surface eddy. The ship

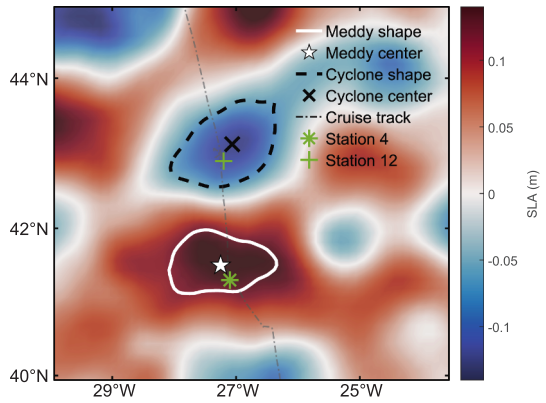

Fig. 6. Sea Level Anomaly map for the 16th of June 2012. The cruise track is represented as a black dash and dotted line. The meddy and the associated eddy centers are identified as a star and an x, respectively, and their contours are identified as a solid white line and a dashed black line, respectively. Station 4 and station 12 are represented as a green asterisk and a green cross respectively.

crossed the MAR at approximately 57°N (Fig. 1). Northwest of the MAR, intensive fluctuations suggest the presence of the Irminger Current and strong eddy activity. Note that the current velocity at 0–400 m clearly exceeds that at 400–800 m depth, practically everywhere except between 41 and 42°N. In these latitudes, where the deep meddy core is registered, velocities at 400–800 m depth exceed those in the upper ocean.

Both surface signals of the meddy and the cyclone were tracked back in time using AMEDA (Fig. 8). From the 16th of June 2012, the meddy surface signal was tracked back for about 3 years, to the 9th of August 2009. Associating this track with the meddy translation across the region, we conclude that, from August 2009 to March 2010, the meddy was stationary above Gloria Seamount (at 45.44N, 15.69W). Afterwards, it predominantly travelled southwest, parallel to the Azores-Biscay Rise, crossing the southeastern end of the King's Trough, until it reached approximately 43N, 24W, where it became stationary again from October to November 2011. After that, the meddy traveled west-

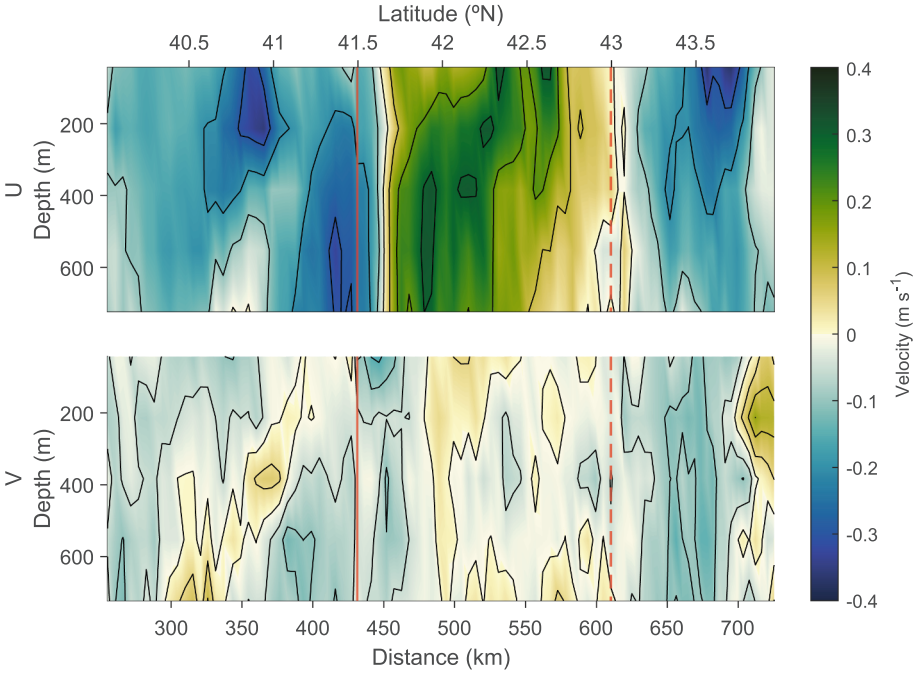

Fig. 5. Vertical section of the ADCP data showing velocity measurements in the zonal (U) and meridional (V) components. Both components are referenced along distance (bottom) and along latitude (top). Stations 4 and 12 are represented as a red line and a red dashed line, respectively.

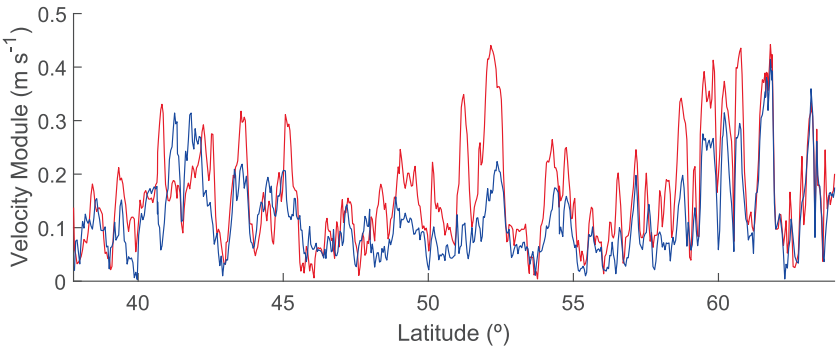

Fig. 7. Absolute values of ADCP current velocities, averaged in the layer 0—400 m (red line) and in the layer 400–800 m (blue line).

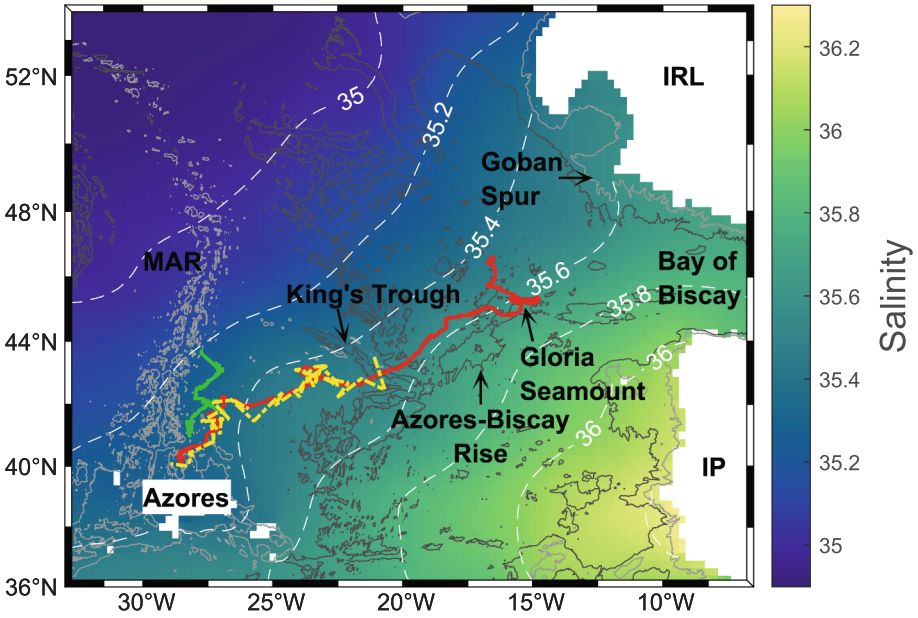

Fig. 8. Map of salinity at 1000 m for the study area, with salinity contours represented as white dashed lines. Bathymetry for 2000 and 4000 m is represented as light gray and dark gray lines, respectively. The red line represents the track of the meddy, the green line represents the track of the cyclonic eddy using altimetry data, and the yellow dashed line represents the track of Argo n°6900650. The main locations and geographical features are identified: IRL (Ireland), IP (Iberian Peninsula), Azores, Bay of Biscay, MAR (Mid-Atlantic Ridge), Goban Spur, King's Trough, Gloria Seamount, Azores-Biscay Rise.

southwest until it met the cyclonic eddy. Being coupled, both eddies moved south and southwest along the MAR. The forward track suggests the last recorded meddy position at 40.13N, 28.56W on November 11, 2012. The track lasted 3 years and 3 months and covers around 3300 km.

To prove that the track, derived following its surface anticyclone with AMEDA, corresponds to a meddy, we found an Argo (n°6900650) that drifted along this track from the 4th of February 2011 to the 5th of November 2012 (Fig. 8). The temperature and salinity anomalies of the Argo profiles relative to MEDTRANS climatology exceeded 1°C in temperature and 0.2 in salinity in the 800–1250 m depth range (Fig. 3) and show a very similar signature to that of the meddy at station 4 (Fig. 4). This suggests that the derived trajectory really followed the meddy during at least 22 months of Argo observations (Fig. 8).

The backtracking of the cyclonic eddy allows its first observation on the 13th of May 2012 at 43.69N, 27.69W (Fig. 8). The eddy traveled south along the MAR as far south as 40.94N, 28.19W on the 16th of January 2013, when its track was lost. The lifetime of this cyclonic eddy was 8 months, during which it covered over 1000 km.

According to AMEDA results, during its travel, the meddy surface signal was characterized by an average azimuthal velocity of 18 cm s^{-}1 with the maximum recorded value of 25 cm s^{-}1, and an average radius of 51 km with a maximum of 93 km. The radius of the meddy, derived from ship ADCP data, was defined as enclosed by the outer (+/-)20 cm s^{-1} contours around station 4, and compared with the mean azimuthal velocity and radius derived from AMEDA for the same day (Table 1). An underestimation of the current velocity, typical for altimetry data (Bashmachnikov, Neves, Calheiros, et al., 2015) results in a smaller Rossby number $Ro = V/fR$. Here, f is the Coriolis parameter. Still, both are of the same order of magnitude, which suggests a reliability of the satellite derived results (Mkhinini et al., 2014). A general trend of decreasing azimuthal velocity over time and an increasing radius of the meddy surface signal is detected (Fig. 9). After August 26, 2012, both velocity and radius experienced more pronounced strong variations. An accelerating decay in the mean values suggests dissipation of a meddy

Table 1
Comparison between the azimuthal velocity (V), corresponding radius (R), and respective vortex Rossby number (Ro) computed from AMEDA (on the 16th of June 2012) and retrieved from the ADCP.

	AMEDA	ADCP
V (cm s^{-1})	11	21
R (km)	57	69
ro	0.02	0.03

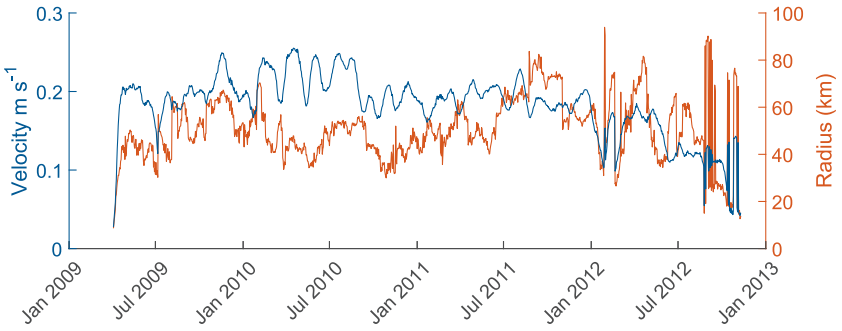

Fig. 9. Velocity (blue) and radius (orange) of the meddy throughout its lifetime, computed by AMEDA.

below.

Based on the average radius and translation velocity from AMEDA, and the height inferred from the CTD, the meddy's transport was, on average, 1.7 Sv throughout its track. Considering the maximum core salinity from the Argo buoy and its temperature profiles, it was estimated that this meddy transported 2.6×10^{11} tons of salt, with a heat flux of 60 ± 2 TW.

4. Discussion

The CTD data from the NA-VICE cruise, combined with Argo float data (No. 6900650), revealed the presence of a meddy with its core located between 800 and 1400 m depth. This feature is characterized by a salinity anomaly exceeding 0.2 and a temperature anomaly greater than 2°C relative to MEDTRANS climatology (Fig. 3), together with a negative anomaly in the Brunt-Väisälä frequency, which is typical of well-mixed meddy cores. While some studies have suggested a decoupling between the thermohaline structure and chemical properties (e.g., oxygen and nutrient concentrations) in certain meddies (Brogueira et al., 2004), the meddy observed in this study does not exhibit such a separation. Instead, the deep oxygen minimum is well aligned with the depth range of the salinity maximum, indicating a coherent coupling between physical and biogeochemical signatures within the eddy core. The ADCP data confirm that the influence of the meddy extends throughout the water column up to the surface (Fig. 5), consistent with the findings of Käse & Zenk (1987). However, the observed shift in the axis of rotation within the upper 400 m suggests a partial decoupling between the meddy core and its surface expression, previously described in Bashmachnikov et al. (2013).

Unlike station 4, where salinity increases gradually with depth, the salinity and temperature increase at station 12 is abrupt and confined to a relatively narrow depth range (Fig. 2a, b). The water mass characteristics of MW at station 4 overlap with those observed at station 12 (Fig. 4). The two stations are separated by 160 km, a distance that significantly exceeds the typical meddy radius, which at these latitudes is comparable to the radius of the meddy surface expression (Bashmachnikov et al., 2014). This suggests that at station 12, and in the close vicinity of the center of a strong cyclone, a portion of MW may have been detached from the main meddy core due to cyclonic interaction. A concurrent increase in the surface signal radius and a decrease in azimuthal velocity, together with the structure of the meddy core, support this interpretation and may indicate a stage of meddy decay. The dynamical intensity of meddy surface signatures signals is known to respond sensitively to changes in meddy radius, as shown by Bashmachnikov & Carton (2012) and Bashmachnikov et al. (2014). Thus, the observations may point to an additional mechanism contributing to meddy decay—namely, interaction with strong surface cyclones—which has not been explicitly documented in previous literature.

The trajectory of the meddy surface signal was backtracked over a period exceeding three years using the AMEDA algorithm (Fig. 8). The presence of a subsurface meddy is further supported by approximately two years of Argo observations (float n°6900650), which closely followed the trajectory of the surface signal for more than half of the reconstructed path. The results indicate that the meddy predominantly propagated southwestward with an average translation velocity of 0.03 m s^{-1}, consistent with previous studies (Richardson et al., 2000).

The reconstructed path suggests that interactions with topographic features, such as seamounts, may lead to periods of reduced propagation speed or quasi-stationary behavior. The time series of the meddy surface radius (Fig. 9) exhibits an initial increasing trend during the early stage of the meddy lifetime, consistent with Ienna et al. (2022), followed by a gradual decrease after 2012, suggesting an overall decay phase. The azimuthal velocity remains relatively stable initially but begins to decrease after 2012.

In addition to the previously discussed interaction with a surface cyclone, the encounter with the Mid-Atlantic Ridge (MAR) in the second half of 2012 likely contributed to the meddy's decay. The estimated volume, salinity, and heat transports are consistent with values reported in previous studies (Bashmachnikov, Neves, Calheiros, et al., 2015; Shapiro et al., 1994).

Although the Argo float only tracked the meddy from about halfway through its lifetime, we assume that the full trajectory reconstructed using the AMEDA algorithm is reliable. This implies that the meddy formation site was, most likely, located along the southern part of the Irish continental shelf. The concept of meddy formation in the northern Atlantic is relatively recent. Prior to 2000, such structures were often described as "meddy-like," and even in more recent studies, generation sites are rarely identified north of Cape Finisterre or Cape Ortegal. Meddies observed north of 43°N have generally been assumed to originate from the northern Iberian margin and propagate northwestward (Bashmachnikov, Neves, Calheiros, et al., 2015; Richardson et al., 1991, 2000). However, the MW undercurrent is known to extend farther north along the Bay of Biscay and the southwestern Irish shelf (Iorga & Lozier, 1999a, 1999b). Prominent topographic features, such as the Goban Spur on the northern side of the Bay of Biscay, may exert a similar dynamical influence on the MOW as the Gulf of Cadiz near Cape São Vicente (Ambar et al., 2008; Barbosa Aguiar et al., 2013; Carton et al., 2013; Serra et al., 2002). Meddies are known to preserve the thermohaline properties of their formation regions within their cores over timescales of several years (Armi et al., 1989; Bashmachnikov, Neves, Calheiros, et al., 2015; Richardson et al., 2000), while these properties evolve along the Mediterranean Undercurrent as it progresses northward (Ambar et al., 2002; Iorga & Lozier, 1999a, 1999b; Mauritzen et al., 2001). The thermohaline properties of the meddy core observed in this study, featuring a peak salinity of 35.55 and a temperature of 9.79°C at depths of 1000–1100 m, closely match MOW properties reported for the Goban Spur region (Iorga & Lozier, 1999a, 1999b). Furthermore, Shoosmith et al. (2005) documented meddy formation in the Goban Spur and Porcupine Seabight region, supporting the interpretation that this area may serve as a previously underrecognized formation site.

Therefore, we suggest that a subset of meddies observed north of the Azores might originate along the Irish continental shelf. If confirmed,

these features would represent an additional source of modified MW in the northeastern North Atlantic, contributing to the transport of heat, salt, and biogeochemical properties from the eastern boundary. Improved understanding of their formation and evolution is thus essential for accurately characterizing both the physical structure and biogeochemical dynamics of intermediate waters in this region.

5. Conclusions

A meddy was identified at 41.3N, 27.1W between 400–1400 m depth on the 16th of June 2012 during the NAVICE cruise (KN207-03), based on the thermohaline criteria of Richardson et al. (1991) and Bashmachnikov, Neves, Calheiros, et al. (2015). The meddy exhibits a clear anticyclonic signature, with a radius of approximately 60 km and azimuthal current velocities reaching up to 38 cm s^{-1}, as derived from ADCP measurements. The meddýs surface signal interacted with a strong surface cyclone, forming a dipole pair that persisted for several months, as revealed by backtracking CMEMS altimetry data using the AMEDA algorithm. During the observation period, this interaction led to the entrainment of MW beneath the cyclone, likely representing a detached MW fragment originating from the meddy core. Subsequent tracking of the meddy surface signal indicates a gradual decrease in both radius and intensity (azimuthal velocity), consistent with the decay of the underlying meddy reported in previous studies. These observations suggest a potential additional mechanism of meddy decay—namely, interaction with strong surface cyclones.

The meddy was tracked for approximately 3.3 years using CMEMS altimetry data, with a substantial portion of its trajectory corroborated by observations from an Argo float trapped within the eddy. Over this period, the meddy traveled more than 3300 km, predominantly moving southwestward at an average velocity of 0.03 m s^{-1}. The reconstructed trajectory, together with the thermohaline characteristics of the meddy core, supports the hypothesis that the eddy originated along the Irish continental shelf, likely in the vicinity of the Goban Spur. Future studies should further investigate the Goban Spur and other regions of the Irish shelf as potential meddy generation sites, as well as their contribution to the formation of the Mediterranean salt tongue in the North Atlantic.

CRediT authorship contribution statement

Tiago Serpa: Writing – original draft, Methodology, Formal analysis, Data curation, Conceptualization. **Igor Bashmachnikov:** Writing – review & editing, Methodology, Formal analysis, Conceptualization. **Paulo Relvas:** Writing – review & editing, Supervision. **Ana Martins:** Writing – review & editing, Supervision, Resources, Formal analysis, Conceptualization.

Declaration of competing interest

The authors declare that they have no known competing financial interests or personal relationships that could have appeared to influence the work reported in this paper.

Acknowledgements

The authors wish to express their gratitude to Dr Kay Bidle (Rutgers University, USA), principal investigator of the international project NAVICE*: Lipid lubrication of oceanic carbon and sulphur biogeochemistry via a host–virus chemical arms race* (Ref. No. OCE-1061883, funded by the NSF), for kindly providing *in situ* datasets obtained during the R/V *Knorr* cruise KN207-03, which took place from the Azores to Iceland in the summer of 2012. OKEANOS research unit received national funds through the FCT - Fundação para a Ciência e Tecnologia, I.P. by project reference UID/05634/2025 (DOI: 10.54499/UID/05634/2025), and from the Regional Directorate for Science, Innovation and Development of the Azores Government through the PROSCIENTIA Incentive System under project M1.1.A/FUNC.UI&D/014/2025. Additional funding for this study was provided by the international project MAGAL Constellation – *Defining the pillar of a future constellation for monitoring the Ocean and Climate Change* (Ref. ACORES-01-0145-FEDER-000129), through the primary beneficiary entity Fundação Gaspar Frutuoso (University of the Azores), by the COAST project funded under the 2020–2021 Biodiversa and Water JPI joint call for research projects, within the BiodivRestore ERA-NET Cofund (GA No. 101003777), and by the Estagiar L programme funded by the Regional Government of the Azores through IMAR – Instituto do Mar (University of the Azores).

Data availability

Data will be made available on request. https://doi.org/10.7284/900540 (Reference data) (Rolling Deck to Repository (R2R))

References

Ambar, I., Serra, N., Brogueira, M.J., Cabeçadas, G., Abrantes, F., Freitas, P., Gonçalves, C., Gonzalez, N., 2002. Physical, chemical and sedimentological aspects of the Mediterranean outflow off Iberia. Deep Sea Res. Part II 49 (19), 4163–4177. https://doi.org/10.1016/S0967-0645(02)00148-0.

Ambar, I., Serra, N., Neves, F., Ferreira, T., 2008. Observations of the mediterranean undercurrent and eddies in the gulf of Cadiz during 2001. J. Mar. Syst. 71 (1–2), 195–220. https://doi.org/10.1016/j.jmarsys.2007.07.003.

Arhan, M., Colin De Verdiére, A., Mémery, L., 1994. The Eastern boundary of the subtropical north Atlantic. J. Phys. Oceanogr. 24 (6), 1295–1316. https://doi.org/10.1175/1520-0485(1994)024<1295:TEBOTS>2.0.CO;2.

Armi, L., Stommel, H., 1983. Four Views of a Portion of the North Atlantic Subtropical Gyre. https://journals.ametsoc.org/view/journals/phoc/13/5/1520-0485_1983_013_0828_fvoapo_{20}_co_2.xml.

Armi, L., Zenk, W., 1984. Large lenses of highly saline Mediterranean water. J. Phys. Oceanogr. 14 (10), 1560–1576. https://doi.org/10.1175/1520-0485(1984)014<1560:LLOHSM>2.0.CO;2.

Armi, L., Hebert, D., Oakey, N., Price, J.F., Richardson, P.L., Rossby, H.T., Ruddick, B., 1989. Two years in the life of a Mediterranean salt lens. J. Phys. Oceanogr. 19 (3), 354–370. https://doi.org/10.1175/1520-0485(1989)019<0354:TYITLO>2.0.CO;2.

Barbosa Aguiar, A.C., Peliz, Á., Carton, X., 2013. A census of Meddies in a long-term high-resolution simulation. Prog. Oceanogr. 116, 80–94. https://doi.org/10.1016/j.pocean.2013.06.016.

Bashmachnikov, I., Carton, X., 2012. Surface signature of Mediterranean water eddies in the Northeastern Atlantic: effect of the upper ocean stratification. Ocean Sci. 8 (6), 931–943. https://doi.org/10.5194/os-8-931-2012.

Bashmachnikov, I., Machín, F., Mendonça, A., Martins, A., 2009a. In situ and remote sensing signature of meddies east of the mid-Atlantic ridge. J. Geophys. Res. Oceans 114 (C5), 2008JC005032. https://doi.org/10.1029/2008JC005032.

Bashmachnikov, I., Mohn, C., Pelegrí, J.L., Martins, A., Jose, F., Machín, F., White, M., 2009b. Interaction of Mediterranean water eddies with Sedlo and Seine Seamounts, Subtropical Northeast Atlantic. Deep Sea Res. Part II 56 (25), 2593–2605. https://doi.org/10.1016/j.dsr2.2008.12.036.

Bashmachnikov, I., Boutov, D., Dias, J., 2013. Manifestation of two meddies in altimetry and sea-surface temperature. Ocean Sci. 9 (2), 249–259. https://doi.org/10.5194/os-9-249-2013.

Bashmachnikov, I., Carton, X., Belonenko, T.V., 2014. Characteristics of surface signatures of Mediterranean water eddies. J. Geophys. Res. Oceans 119 (10), 7245–7266. https://doi.org/10.1002/2014JC010244.

Bashmachnikov, I., Neves, F., Calheiros, T., Carton, X., 2015a. Properties and pathways of Mediterranean water eddies in the Atlantic. Prog. Oceanogr. 137, 149–172. https://doi.org/10.1016/j.pocean.2015.06.001.

Bashmachnikov, I., Neves, F., Nascimento, Â., Medeiros, J., Ambar, I., Dias, J., Carton, X., 2015b. Temperature–salinity distribution in the northeastern Atlantic from ship and Argo vertical casts. Ocean Sci. 11 (2), 215–236. https://doi.org/10.5194/os-11-215-2015.

Bashmachnikov, I., Raj, R.P., Golubkin, P., Kozlov, I.E., 2023. Heat transport by mesoscale eddies in the Norwegian and greenland seas. J. Geophys. Res. Oceans 128 (2), e2022JC018987. https://doi.org/10.1029/2022JC018987.

Bower, A.S., Serra, N., Ambar, I., 2002. Structure of the Mediterranean Undercurrent and Mediterranean Water spreading around the southwestern Iberian Peninsula. J. Geophys. Res. Oceans 107 (C10). https://doi.org/10.1029/2001JC001007.

Brogueira, M.J., Cabeçadas, G., Gonçalves, C., 2004. Chemical resolution of a meddy emerging off southern Portugal. Cont. Shelf Res. 24 (15), 1651–1657. https://doi.org/10.1016/j.csr.2004.05.012.

Carton, X., Chérubin, L., Paillet, J., Morel, Y., Serpette, A., Le Cann, B., 2002. Meddy coupling with a deep cyclone in the Gulf of Cadiz. J. Mar. Syst. 32 (1–3), 13–42. https://doi.org/10.1016/S0924-7963(02)00028-3.

Carton, X., Le Cann, B., Serpette, A., Dubert, J., 2013. Interactions of surface and deep anticyclonic eddies in the Bay of Biscay. J. Mar. Syst. 109–110, S45–S59. https://doi.org/10.1016/j.jmarsys.2011.09.014.

Copernicus Marine Service. (2024). *European Seas Gridded L4 Sea Surface Heights And Derived Variables Reprocessed [Data set]*. doi:10.48670/moi-00141.

Daniault, N., Mazé, J.P., Arhan, M., 1994. Circulation and mixing of Mediterranean water west of the Iberian Peninsula. Deep Sea Res. Part I 41 (11–12), 1685–1714. https://doi.org/10.1016/0967-0637(94)90068-X.

De Pascual-Collar, Á.G., Sotillo, M., Levier, B., Aznar, R., Lorente, P., Amo-Baladrón, A., Álvarez-Fanjul, E., 2019. Regional circulation patterns of Mediterranean Outflow Water near the Iberian and African continental slopes. Ocean Sci. 15 (3), 565–582. https://doi.org/10.5194/os-15-565-2019.

Gasser, M., Pelegrí, J.L., Emelianov, M., Bruno, M., Gràcia, E., Pastor, M., Peters, H., Rodríguez-Santana, Á., Salvador, J., Sánchez-Leal, R.F., 2017. Tracking the Mediterranean outflow in the Gulf of Cadiz. Prog. Oceanogr. 157, 47–71. https://doi.org/10.1016/j.pocean.2017.05.015.

Hogg, N.G., Stommel, H.M., 1990. How currents in the upper thermocline could advect meddies deeper down. Deep Sea Res. Part A 37 (4), 613–623. https://doi.org/10.1016/0198-0149(90)90093-B.

Hummon, J.M., Firing, E., 2003. A direct comparison of two RDI shipboard ADCPs: a 75-kHz ocean surveyor and a 150-kHz Narrow Band*. J. Atmos. Oceanic Tech. 20 (6), 872–888. https://doi.org/10.1175/1520-0426(2003)020<0872:ADCOTR>2.0.CO;2.

Ienna, F., Jo, Y.-H., Yan, X.-H., 2014. A new method for tracking meddies by satellite altimetry. J. Atmos. Oceanic Tech. 31 (6), 1434–1445. https://doi.org/10.1175/JTECH-D-13-00080.1.

Ienna, F., Bashmachnikov, I., Dias, J., 2022. Meddies and their sea surface expressions: observations and theory. J. Phys. Oceanogr. 52 (11), 2643–2656. https://doi.org/10.1175/JPO-D-22-0081.1.

Iorga, M.C., Lozier, M.S., 1999a. Signatures of the Mediterranean outflow from a North Atlantic climatology: 1. Salinity and density fields. J. Geophys. Res. Oceans 104 (C11), 25985–26009. https://doi.org/10.1029/1999JC900115.

Iorga, M.C., Lozier, M.S., 1999b. Signatures of the Mediterranean outflow from a North Atlantic climatology: 2. Diagnostic velocity fields. J. Geophys. Res. Oceans 104 (C11), 26011–26029. https://doi.org/10.1029/1999JC900204.

Jungclaus, J.H., 1999. A three-dimensional simulation of the formation of anticyclonic lenses (Meddies) by the instability of an intermediate depth boundary current. J. Phys. Oceanogr. 29 (7), 1579–1598. https://doi.org/10.1175/1520-0485(1999)029<1579:ATDSOT>2.0.CO;2.

Käse, R.H., Zenk, W., 1987. Reconstructed mediterranean salt lens trajectories. J. Phys. Oceanogr. 17 (1), 158–163. https://doi.org/10.1175/1520-0485(1987)017<0158:RMSLT>2.0.CO;2.

Le Vu, B., Stegner, A., Arsouze, T., 2018. Angular momentum eddy detection and tracking algorithm (AMEDA) and its application to coastal eddy formation. J. Atmos. Oceanic Tech. 35 (4), 739–762. https://doi.org/10.1175/JTECH-D-17-0010.1.

Maas, L.R.M., Zahariev, K., 1996. An exact, stratified model of a meddy. Dyn. Atmos. Oceans 24 (1–4), 215–225. https://doi.org/10.1016/0377-0265(95)00451-3.

Mauritzen, C., Morel, Y., Paillet, J., 2001. On the influence of Mediterranean Water on the Central Waters of the North Atlantic Ocean. Deep Sea Res. Part I 48 (2), 347–381. https://doi.org/10.1016/S0967-0637(00)00043-1.

McDougall, T. J., Barker, P. M., 2011. Getting started with TEOS-10 and the Gibbs Seawater (GSW) Oceanographic Toolbox (p. 28). SCOR/IAPSO WG127.

McDougall, T.J., Jackett, D.R., Millero, F.J., Pawlowicz, R., Barker, P.M., 2012. A global algorithm for estimating absolute Salinity. Ocean Sci. 8 (6), 1123–1134. https://doi.org/10.5194/os-8-1123-2012.

Mcwilliams, J.C., 1984. The emergence of isolated coherent vortices in turbulent flow. J. Fluid Mech. 146, 21–43. https://doi.org/10.1017/S0022112084001750.

Mkhinini, N., Coimbra, A.L.S., Stegner, A., Arsouze, T., Taupier-Letage, I., Béranger, K., 2014. Long-lived mesoscale eddies in the eastern Mediterranean Sea: analysis of 20 years of AVISO geostrophic velocities. J. Geophys. Res. Oceans 119 (12), 8603–8626. https://doi.org/10.1002/2014JC010176.

Ochoa, J., Bray, N.A., 1991. Water mass exchange in the Gulf of Cadiz. Deep Sea Res. Part A 38, S465–S503. https://doi.org/10.1016/S0198-0149(12)80021-5.

Oliveira, P. B., Serra, N., Fiúza, A. F. G., Ambar, I., 2000. Chapter 7 A study of meddies using simultaneous in-situ and satellite observations. In Elsevier Oceanography Series (Vol. 63, pp. 125–148). Elsevier. 10.1016/S0422-9894(00)80008-2.

Pingree, R.D., Le Cann, B., 1993a. A shallow meddy (a smeddy) from the secondary Mediterranean salinity maximum. J. Geophys. Res. Oceans 98 (C11), 20169–20185. https://doi.org/10.1029/93JC02211.

Pingree, R.D., Le Cann, B., 1993b. Structure of a meddy (Bobby 92) southeast of the Azores. Deep Sea Res. Part I 40 (10), 2077–2103. https://doi.org/10.1016/0967-0637(93)90046-6.

Prater, M. D., Sanford, T. B., 1994. A Meddy off Cape St. Vincent. Part I: Description. J. Phys. Oceanogr. 24(7), 1572–1586. 10.1175/1520-0485(1994)024<1572:AMOCSV>2.0.CO;2.

Richardson, P.L., Tychensky, A., 1998. Meddy trajectories in the Canary Basin measured during the SEMAPHORE experiment, 1993–1995. J. Geophys. Res. Oceans 103 (C11), 25029–25045. https://doi.org/10.1029/97JC02579.

Richardson, P.L., Price, J.F., Walsh, D., Armi, L., Schröder, M., 1989. Tracking three meddies with SOFAR floats. J. Phys. Oceanogr. 19 (3), 371–383. https://doi.org/10.1175/1520-0485(1989)019<0371:TTMWSF>2.0.CO;2.

Richardson, P.L., McCartney, M.S., Maillard, C., 1991. A search for meddies in historical data. Dyn. Atmos. Oceans 15 (3–5), 241–265. https://doi.org/10.1016/0377-0265(91)90022-8.

Richardson, P.L., Bower, A.S., Zenk, W., 2000. A census of Meddies tracked by floats. Prog. Oceanogr. 45 (2), 209–250. https://doi.org/10.1016/S0079-6611(99)00053-1.

Serra, N., Ambar, I., 2002. Eddy generation in the Mediterranean undercurrent. Deep Sea Res. Part II 49 (19), 4225–4243. https://doi.org/10.1016/S0967-0645(02)00152-2.

Serra, N., Sadoux, S., Ambar, I., Renouard, D., 2002. Observations and laboratory modeling of meddy generation at cape St Vincent. J. Phys. Oceanogr. 32 (1), 3–25. https://doi.org/10.1175/1520-0485(2002)032<0003:OALMOM>2.0.CO;2.

Shapiro, G., Zenk, W., Meschanov, S., Tokos, K., Meschanov, S., Tokos, K., 1994. Self-similarity of the meddy family in the eastern north-atlantic. Oceanol. Acta 18 (1), 29–42.

Shoosmith, D.R., Richardson, P.L., Bower, A.S., Rossby, H.T., 2005. Discrete eddies in the northern North Atlantic as observed by looping RAFOS floats. Deep Sea Res. Part II 52 (3–4), 627–650. https://doi.org/10.1016/j.dsr2.2004.12.011.

Stammer, D., Hinrichsen, H., Käse, R.H., 1991. Can meddies be detected by satellite altimetry? J. Geophys. Res. Oceans 96 (C4), 7005–7014. https://doi.org/10.1029/90JC02740.

Zhang, Z., Wang, W., Qiu, B., 2014. Oceanic mass transport by mesoscale eddies. Science 345 (6194), 322–324. https://doi.org/10.1126/science.1252418.